NANO LETTERS
Letter
Cite This: Nano Lett. 2018, 18, 7441−7447
pubs.acs.org/NanoLett

Tuning the Relaxation of Nanopatterned Polymer Films with Polymer-Grafted Nanoparticles: Observation of Entropy−Enthalpy Compensation

Sonal Bhadauriya,[†] Xiaoteng Wang,[†] Praveen Pitliya,[‡] Jianan Zhang,[§] Dharmaraj Raghavan,[‡] Michael R. Bockstaller,[§] Christopher M. Stafford,[∥] Jack F. Douglas,*[,∥] and Alamgir Karim*[,†]

[†]Department of Polymer Engineering, University of Akron, Akron, Ohio 44325 United States
[‡]Department of Chemistry, Howard University, Washington, District of Columbia 20059, United States
[§]Department of Materials Science and Engineering, Carnegie Mellon University, Pittsburgh, Pennsylvania 15213, United States
[∥]Materials Science and Engineering Division, National Institute of Standards and Technology, Gaithersburg, Maryland 20899, United States

Supporting Information

ABSTRACT: Polymer films provide a versatile platform in which complex functional relief patterns can be thermally imprinted with a resolution down to few nanometers. However, a practical limitation of this method is the tendency for the imprinted patterns to relax ("slump"), leading to loss of pattern fidelity over time. While increasing temperature above glass transition temperature (T_g) accelerates the slumping kinetics of neat films, we find that the addition of polymer-grafted nanoparticles (PGNP) can greatly enhance the thermal stability of these patterns. Specifically, increasing the concentration of poly(methyl methacrylate) (PMMA) grafted titanium dioxide (TiO_2) nanoparticles in the composite films slows down film relaxation dynamics, leading to enhanced pattern stability for the temperature range that we investigated. Interestingly, slumping relaxation time is found to obey an entropy−enthalpy compensation (EEC) relationship with varying PGNP concentration, similar to recently observed relaxation of strain-induced wrinkling in glassy polymer films having variable film thickness. The compensation temperature, T_{comp} was found to be in the vicintity of the bulk T_g of PMMA. Our results suggest a common origin of EEC relaxation in patterned polymer thin films and nanocomposites.

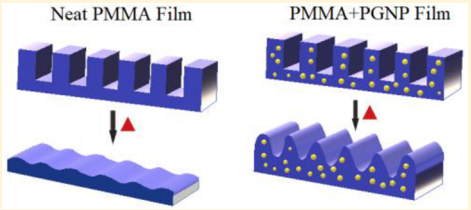

KEYWORDS: *Polymer nanocomposite, pattern decay, stability, lithography, enthalpy−entropy compensation effect, polymer thin films*

Controlling the stability of relief patterns in polymer thin films presents an important problem from both fundamental and applications standpoint. Surface patterns are utilized in various applications such as lithography,[1] nanodevices,[2] optical diffusers,[3] and biosensors[4] where a decay in the stability of these structures can render them unusable. The stability of imprinted nanostructures in homopolymer films has been extensively studied, using both ex situ[5−7] and in situ[8−11] techniques. For low molecular mass unentangled polymer films, the decay of imprinted nanostructures, termed "slumping", is governed by Laplace pressure induced viscous flow[6,7] so that residual stress effects arising in nanoimprinted high molecular mass films are not a complication.[6,9,10] For unentangled polymer films, the rate of slumping is governed by the film viscosity[6−8,10] and hence measurements of slumping rate for films both with and without polymer brush grafted nanoparticles (PGNPs) should allow for direct estimates of how the PGNP influence the relaxation time and viscosity of polymer films near the glass transition temperature, T_g.

Previous work has shown that molecular additives can effectively stabilize nanoimprinted patterns,[12] and it is natural to investigate whether PGNPs can serve this purpose given the significant influence nanoparticles have on the properties of nanocomposite materials.[13] Polymer nanocomposites offer vast possibilities for creating new functional materials through the control of the size and organization of the PGNP within the polymer matrix,[14] enabling the tuning of the flow properties,[15] glass transition,[16] relaxation dynamics,[17] supression of dewetting,[18] and effective mechanical strength[19] for the resultant nanocomposite material. Previous studies demonstrated that addition of PGNP to a polymer matrix can significantly affect the glass transition of the nanocomposite[16] and also revealed a tendency of imprinting to influence the distribution of the PGNPs under strong confinement conditions.[20] Relaxation behavior of PGNP nanocomposite system essentially depends on the grafted chain-matrix chain interactions, grafting density, and size of the PGNP. The effect of PGNPs in imparting structural stability is essentially unexplored.

We investigate the slumping effect in imprinted poly(methyl methacrylate) (PMMA) (M_n = 3.1 kg/mol, where M_n is the

Received: June 20, 2018
Revised: September 26, 2018
Published: November 6, 2018

DOI: 10.1021/acs.nanolett.8b02514
Nano Lett. 2018, 18, 7441−7447

number-average molecular mass) thin films containing PMMA (M_n = 15 kg/mol) grafted titania (TiO_2 PGNP). TiO_2 PGNP had an average diameter of 29.9 (±6.6) nm after grafting with chain density ≈0.907 chains/nm^2. The grafted PMMA chains in this study have a molecular mass that is higher than the matrix molecular mass, corresponding to the so-called "wet brush" regime[21] where the grafted chains are expected to be swollen by the polymer matrix chains. Addition of PGNP significantly improved the thermal stability above T_g and these additives act as stabilizing agents for the patterned nanostructures. As the PGNP loading is increased, the patterned nanostructure exhibited a longer relaxation time, indicative of an enhanced pattern stability. The dynamics of the slumping process appear to be similar in nature to recent measurements and simulations of the relaxation of wrinkling patterns in ultrathin glassy polymer films,[22] and we indeed find common trends in the relaxation of these films. We apply a similar theoretical framework to quantify the slumping dynamics of our imprinted PGNP nanocomposite polymer films. Notably, the stabilization of the imprinted nanostructures relates to the slowing down of film relaxation dynamics, where we find an entropy−enthalpy compensation effect in the thermally activated free energy parameters governing the "slumping" of the nanoimprinted patterns as the common feature for wrinkled films in general.

Parallel line and space patterns with height 135 (±2.5) nm and width 353 (±0.5) nm used in our study were generated by using a prepatterned PDMS elastomer to imprint PMMA thin films containing varying concentrations of TiO_2 PGNP by mass relative to the PMMA matrix. Samples after imprinting (PDMS peeled off) had a residual layer thickness of 34 (±5) nm underneath the pattern. The topography of imprinted samples was characterized in terms of pattern height (H) using ex situ atomic force microscopy (AFM) after the samples were subjected to different annealing temperatures (T) and exposure times (t) above the ellipsometry-estimated bulk T_g value of the PMMA matrix, $T_{g,bulk}$ ≈ 97.24 (±0.23) °C (Supporting Information, Figure S1a−h). The AFM images of Figure 1a show a comparison between pattern decay of the pure PMMA film, compared to the significantly better preserved pattern height in PMMA film with 30% TiO_2 PGNP after annealing both the films at 115 °C for 90 min. Notably, the nanocomposite film showed a 94% higher pattern height retention compared to the pure PMMA film. This PGNP stabilization effect was quantified by determining pattern line profiles (from the AFM images) for imprinted pure PMMA film versus the 30% (by mass) TiO_2 PGNP nanocomposite film, as shown in Figure 1b, for various annealing times and temperatures.

The normalized pattern height, $H(t, T)/H_o$, decay curves are shown in Figure 2a−e. While increasing temperature (T) from 110 °C to 130 °C increases pattern height decay rate significantly, increasing PGNP concentration from 5% to 30% by relative mass (with respect to the PMMA matrix) slows down the pattern relaxation rate substantially. Increasing the PGNP concentration increases the relaxation time governing the pattern decay, analyzed in terms of the normalized pattern height decay, for example, for the film in Figure 1b and corresponding Figure 2b, annealed for 60 min at 115 °C containing 30% PGNP by mass, H/H_o ≈ 0.71, whereas in the case of neat PMMA film it is only ≈0.04, indicating a 94% higher pattern height retention in the PGNP nanocomposite film. In general, the kinetic decay curves in Figure 2a−e shows

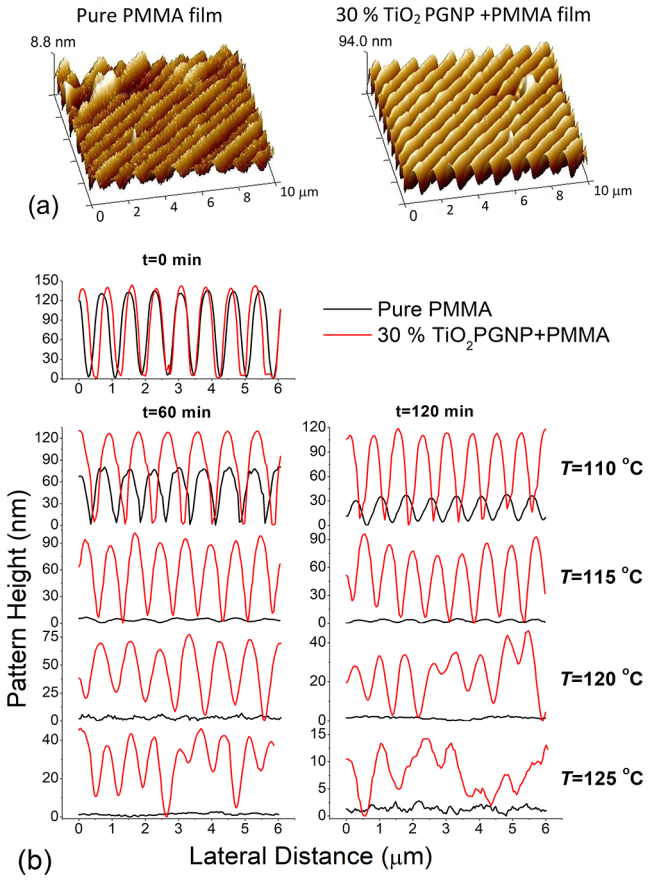

Figure 1. (a) Atomic force microscopy (AFM) images showing the effect of adding TiO_2 PGNP to a PMMA film, after annealing at 115 °C for 90 min where the nanocomposite film displays a 94% higher pattern height retention. TiO_2 PGNP concentration in the nanocomposite film was 30% by mass relative to the PMMA matrix. (b) AFM line profiles comparing the imprinted 0% (pure) and 30% (by mass) TiO_2 PGNP containing PMMA film at 110 °C, 115 °C, 120 °C, and 125 °C for time interval t = 60 min and t = 120 min. The graph at the top depicts the line profiles at t = 0 min.

that for higher PGNP concentrations there is a significant stabilization of the nanoimprinted pattern in comparison to the pure polymer matrix. The decay curves illustrate a non-exponential relaxation behavior and were fitted to a generalized exponential function.[23] Specifically, the normalized pattern height is fit to the following relation,

$$\frac{H}{H_o} \approx \exp[-(t/\tau)^{\beta}] \quad (1)$$

where τ is the pattern relaxation time and β quantifies the degree of non-exponentiality of this relaxation process. There has been much theoretical speculation about β, and we briefly discuss the observed trends for β found in the present slumping study.

In Figure 2f, we observe that β converges to 1 as T increases for a given PGNP concentration. For example, pure PMMA annealed at 110 °C exhibits $\beta \approx 0.85$, whereas the addition of 30% TiO_2 PGNP increases β to a value near 1.5 but both converge to 1 as T increases. It has been previously observed that the relaxation behavior for a polymer nanocomposite exhibits an enhanced rate of relaxation in which $\beta > 1$,[24,25] a relaxation behavior that is not normally observed in glass-forming polymer materials. Recent simulations have shown

DOI: 10.1021/acs.nanolett.8b02514
Nano Lett. 2018, 18, 7441−7447

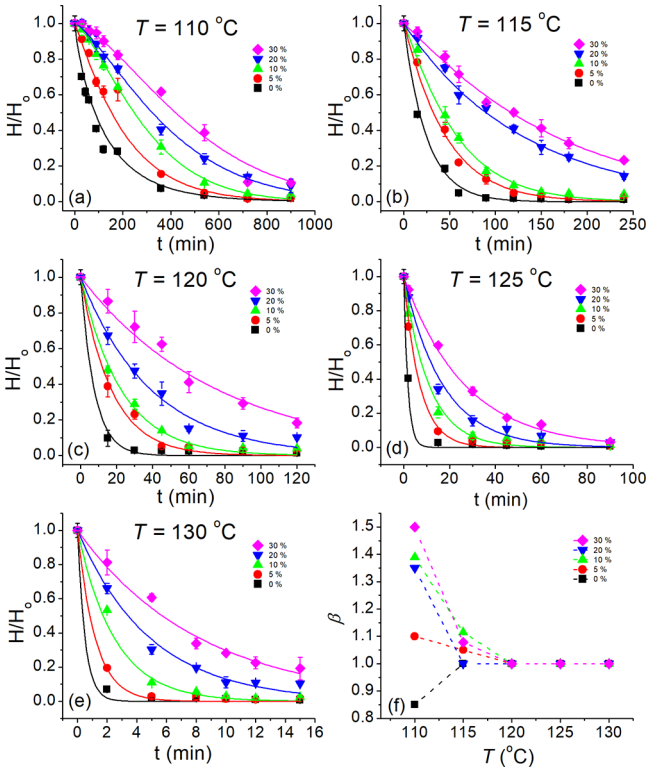

Figure 2. Relaxation dynamics of pattern height for nanoimprinted PMMA thin films containing TiO_2 PGNP (30%, purple diamond; 20%, blue downward arrow; 10%, green upward arrow; 5%, red circle; 0%, black square by mass relative to the PMMA matrix) subjected to slumping measurements at (a) 110 °C, (b) 115 °C, (c) 120 °C, (d) 125 °C, and (e) 130 °C. Solid lines denote fits of eq 1 to the data. The error bars represent one standard deviation of the data, which is taken as the experimental uncertainty of the measurement. (f) Variation of the non-exponential relaxation exponent, β from the slumping relaxation curves as a function of T and different concentrations of TiO_2 PGNP within PMMA matrix.

that nanoparticle clustering in fluids gives rise to this type of "stretched Gaussian" or "compressed exponential" relaxation for large scale structural relaxation as an equilibrium relaxation phenomenon. Chremos and Douglas[24] interpret this phenomenon as arising from the formation of particle clusters and associated local elastic constant fluctuations that drive correlated motion in the fluid in a manner similar to a material with residual stresses.

We directly observe limited PGNP clustering in our system (Supporting Information, Figure S2) under conditions where $\beta > 1$ so that this mechanism seems to offer plausible rationalization of our observations. The limited clustering at low temperature is potentially a result of initial nonequilibrium mold-filling conditions in conjunction with some inhomogeneity of polymer brush grafting density on the nanoparticles. Previous measurements of relaxation in bulk nanocomposite materials have evidenced this type of "anomalous" relaxation.[26] We have verified this interpretation by examining the slumping dynamics of another PGNP additive, PMMA-grafted silica NP (SiO_2 PGNP) to the same polymer material where no overt clustering arises in the cast nanoparticle filled films, either before or after annealing (Supporting Information, Figure S3a–h). SiO_2 PGNP (M_n of the grafted chains ≈19.4 kg/mol) had an average diameter of 7.7 (±2) nm after grafting with an areal density of ≈0.65 chains/nm^2. These well-dispersed systems do not show "stretched Gaussian relaxation" at low temperature, that is, no regime in which $\beta > 1$, consistent with our hypothesis that this phenomenon is associated with PGNP clustering.

Segmental relaxation is normally highly non-Arrhenius in glass-forming polymer liquids above their T_g but temperature dependence is often observed to obey an Arrhenius-type temperature dependence[27−30] allowing for the determination of the activation free energy associated with the relaxation process. The T dependence of the viscosity of polymer liquids tends to be significantly weaker and more Arrhenius-like ("stronger" in the jargon of glass physics),[31] so that an Arrhenius approximation often provides an adequate practical description of polymer viscosity data, at least over a limited temperature range above T_g. This situation appears to apply to nanocomposite pattern slumping data shown in Figure 3 where we plot the relaxation time τ obtained from Figure 2a–e as a function of $1/T$ for different PGNP loadings

$$\tau = \tau_0 \exp(E_a/RT) \quad (2)$$

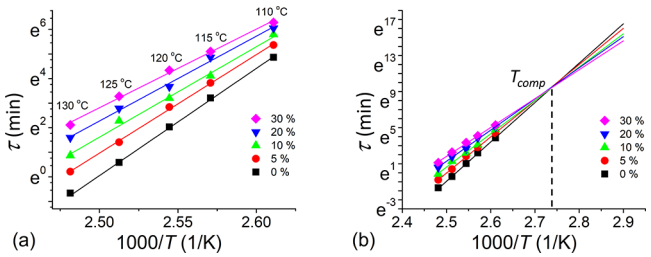

Figure 3. (a) Arrhenius plots for the temperature dependence of the relaxation time (τ). Solid lines show linear Arrhenius fits (eq 2) to the data. (b) Extrapolation of the linear fits leads to a point of convergence, near $T_{comp} \approx 92$ (±5) °C, a T equal to within experimental uncertainty to $T_{g,bulk} \approx 97.24$ (±0.23) °C (see Supporting Information, Figure S1h).

We obtain a reasonably good linear fit ($R^2 \approx 0.99$ for all PGNP conc.) as shown in Figure 3a demonstrating an approximately Arrhenius-type behavior for the pattern relaxation time, as anticipated. The slopes of the curves determine the activation free energy of the relaxation process, which is calculated to be 362 (±10.9) and 266 (±8.54) kJ/mol for slumping in the pure and nanocomposite 30% TiO_2 PGNP filled thin films, where the uncertainty denotes the standard error calculated for the fitted parameter.

We also see from Figure 3b the convergence of the extrapolated relaxation times of both pure and nanocomposite PMMA films near $T \approx 92$ (±5) °C, a temperature essentially coinciding with $T_{g,bulk} \approx 97.24$ (±0.23) °C as measured by ellipsometry (Supporting Information, Figure S1h). Our estimate of uncertainty in the intersection point is obtained graphically by fitting each set of data in Figure 3b to maximum range of compatible slopes, leading to an intersection point range of ±0.4 K^{-1}, corresponding to temperature uncertainty of ±5 °C. At this "compensation" or "isokinetic" temperature, the pattern slumping relaxation time is nearly independent of the PGNP concentration. This characteristic temperature is conventionally called the entropy−enthalpy compensation (EEC) temperature, T_{comp}, where the nanocomposite relaxation is "ideal" in the sense that it is like a material containing no PGNP. A similar behavior has been shown previously in materials with molecular additives,[32,33] rather

DOI: 10.1021/acs.nanolett.8b02514
Nano Lett. 2018, 18, 7441−7447

than PGNP additives. EEC is encountered in the dynamics of many condensed materials[34] and corresponds to a linear dependence between the Arrhenius prefactor, $\ln(\tau_0)$, which scales linearly with the entropy of activation, and the activation enthalpy, E_a. Figure 4a shows that $\ln(\tau_0)$ and E_a indeed

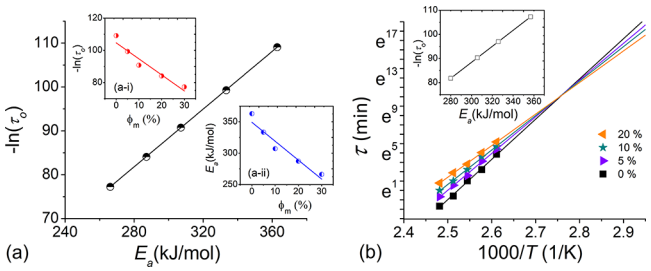

Figure 4. (a) Entropy−enthalpy compensation (EEC) plot for TiO_2 PGNP system (black top-filled circle, $R^2 \approx 0.99$) from nanoimprinted film slumping relaxation data. Insets (a-i) and (a-ii) show $-\ln(\tau_0)$ (red right-half filled circle, $R^2 \approx 0.87$) and E_a (kJ/mol) (blue left-filled circle, $R^2 \approx 0.86$) versus concentration by mass (ϕ_m) of TiO_2 PGNP respectively. (b) Arrhenius plots for the temperature dependence of the relaxation time (τ) for the SiO_2 PGNP (20%, orange left arrow; 10%, blue star; 5%, purple right arrow; 0%, black square), by mass relative to the PMMA matrix. Solid lines show linear Arrhenius fits (eq 2) to the data. Extrapolation of the linear fits leads to a point of convergence, near $T_{comp} \approx 95$ (±3) °C. The inset graph demonstrates the entropy−enthalpy compensation (EEC) plot for SiO_2 PGNP system within PMMA matrix (black hollow square, $R^2 \approx 0.99$).

correlate linearly with each other. Figure 4a-i, a-ii (insets) demonstrate the effect of increasing PGNP concentration which lead to an increase in the entropy of activation, $\ln(\tau_0)$ whereas activation enthalpy, E_a of the process goes down. We see that the increase in entropy of activation of the relaxation process dominates the resultant relaxation behavior of the nanocomposite. In particular, the compensation of the activation enthalpy, E_a with the entropy of activation leads to the observed increase in the relaxation time constant with concentration. Recently, EEC was observed in relaxation dynamics of wrinkled ultrathin polymer films where the activation parameters for the relaxation process were linearly correlated and T_{comp} was found to be about 5 °C below T_g of the bulk material.[22] These observations, and those of the present paper, point toward a common relaxation dynamics origin of the EEC behavior in patterned polymer thin film and nanocomposite systems. We also observe EEC behavior in Figure 4b for the other PGNP additive system (SiO_2 PGNP) where the particles were well dispersed. Figure 4b clearly indicates the convergence of the extrapolated relaxation times of both pure and nanocomposite SiO_2 PGNP films near the compensation temperature, $T_{comp} \approx 95$ (±3) °C, a temperature again close to $T_{g,bulk} \approx 97.24$ (±0.23) °C; see Supporting Information, Figure S1h. Figure 4b (inset graph) shows the linear correlation between $\ln(\tau_0)$ and E_a, explicitly indicating the presence of EEC in the well-dispersed SiO_2 PGNP system as well. Increase in the SiO_2 PGNP concentration lead to an increase in the entropy of activation, $\ln(\tau_0)$ and a decrease in activation enthalpy, E_a (Supporting Information S3k). EEC observed in the relaxation dynamics of imprinted nanocomposite films seems to be independent of the dispersion of the PGNP and it is robustly observed for both the systems investigated, clustered (TiO_2 PGNP) and well-dispersed (SiO_2 PGNP).

The observation of EEC effect is often seen in the relaxation of glass-forming materials.[35] For example, upon adding glycerol to trehalose, the activation energy and activation entropy (log of the relaxation time prefactor of the Johari−Goldstein beta relaxation) both vary in a linear fashion with the concentration of glycerol.[36] EEC is widely observed in the preservation of proteins[37] as the preservation matrix is varied in the hypothermic injury of proteins, cells and tissue,[38] in food preservation[32] and relaxation processes in seeds relevant to desiccation tolerance,[39] biofouling of crude oils[40] and Douglas and co-workers[33,36,37] discuss other applications of EEC to polymeric materials. In a particularly relevant application to the present work, Delcambre et al.[41] have employed a molecular additive to stabilize lithographically etched patterns in thin polymer films and such additives have also been utilized to make polymer films abrasion resistant.[42]

The change in the rate of pattern slumping is quite unlike what one would expect from the changes in the viscosity upon addition of spherical particles to a simple fluid. In particular, Einstein predicted[43] that the shear viscosity of a dilute suspension of spherical particles should increase linearly with particle volume fraction with a temperature independent slope of 2.5. Because the slumping rate should be proportional to the suspension viscosity, the ratio of the slumping rate with the PGNP $[\tau(\phi_v)]$ to the slumping rate without the PGNP $\tau(\phi_v = 0)]$ can be directly compared with Einstein's prediction. In Figure 5, we see that $\tau(\phi_v)/\tau(\phi_v = 0)$ is indeed nearly linear as

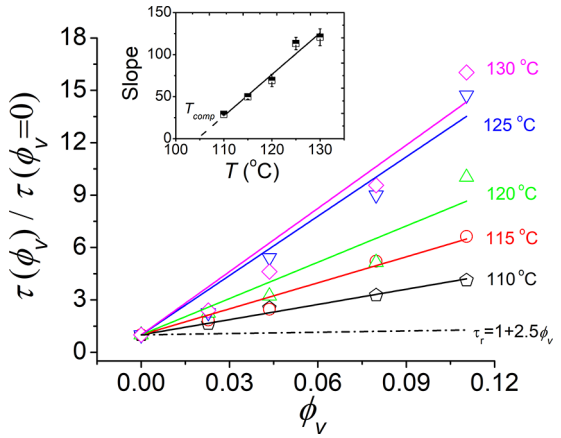

Figure 5. Change of the relaxation time constant of slumping, $\tau(\phi_v)$ as a function of TiO_2 PGNP volume fraction, ϕ_v. The hydrodynamic prediction for spherical particles implies a linear variation of $\tau_r = \tau(\phi_v)/\tau(\phi_v = 0)$ with a slope 2.5, while the observed slope is clearly temperature dependent (110 °C, black open pentagon; 115 °C, red open cirlce; 120 °C, green open upward arrow; 125 °C, blue open downward arrow; 130 °C, purple open diamond). Solid lines denote linear fits to the data. The inset graph (black top-filled square) depicts the temperature dependence of the slope and error bars denotes the standard error of fitting.

one would expect from suspension hydrodynamics but the slope depends strongly on temperature. The inset to Figure 5 shows the T dependence of this slope where the intercept is close to 105 °C, which is somewhat higher than our estimate of T_{comp} from the data in Figure 3b, a deviation that we attribute to the nonlinearity of the data in Figure 5. An appreciable deviation from a linear concentration dependence can be expected even in the viscosity of hard sphere suspensions for volume fractions ϕ_v greater than 0.01 to 0.02[44] so our

DOI: 10.1021/acs.nanolett.8b02514
Nano Lett. 2018, 18, 7441−7447

comparison to the change of the slumping rate based on the Einstein theory is only qualitative, although in line with many engineering studies of particle suspensions[44] where the Einstein theory is compared to experiment over a similar volume fraction range as considered in Figure 5. The systematic curvature of the plots in Figure 5 can be naturally understood from the concentration dependence of the activation energy E_a and the activation entropy, which apart from an additive constant is the log of the prefactor τ_0. In particular, if the activation free-energy is taken to be approximately linear in the nanoparticle concentration (see insets to Figure 4a) then $\tau(\phi_v)/\tau(\phi_v = 0)$ should vary exponentially with ϕ_v and should reduce exactly to unity at $T_{comp.}$ This argument is sufficient to rationalize why the curvature of the plots in Figure 5 becomes more prevalent the further the deviation of T from $T_{comp.}$ We see a similar increased curvature in $\tau(\phi_v)/\tau(\phi_v = 0)$ as T increasingly deviates from T_{comp} arising in the case of SiO_2 PGNP as well, which notably do not exhibit significant aggregation and were quite well dispersed (see Supporting Information, Figure S3a,b). Evidently, the curvature in these plots cannot then be rationalized in terms of particle aggregation.

An important implication of the data trend in Figure 3b is that the stabilizing effect of the PGNP on the imprint patterns should no longer exists if T is lower than T_{comp}, that is, $\tau(\phi_v)/\tau(\phi_v = 0) < 1$. Our data also suggests that the viscosity of the fluid suspension should drop upon adding the nanoparticles, a decidedly noncontinuum effect that has actually been observed in recent measurements of some nanoparticle suspensions.[45,46] Measurements in this regime are highly time-consuming and require a separate study, but we briefly explored whether this effect exists in our imprinted nanocomposite films at $T = 80$ °C (appreciable slumping requiring 2.5 months). We indeed find that the filled imprinted pattern slumps more rapidly compared to the pure PMMA film in the regime below T_{comp} (these preliminary results are described in the Supporting Information, Figure S10). Previous work has also shown that the Johari−Goldstein, or "slow beta" relaxation process measured by high frequency dielectric relaxation, which dominates relaxation in glassy materials, can become shorter with nanoparticles and molecular additives, for example, the addition of fullerene to polyisoprene melts[47] and the addition of polychlorinated biphenyl to polycarbonate.[33]

In summary, the addition of PGNP to thin PMMA films leads to a significant stabilization of nanoimprinted patterns (above T_{comp}) and provide a simple strategy to control high-temperature nanostructural integrity in patterned polymer films. The relaxation dynamics of the imprinted patterns show a clear entropy−enthalpy compensation effect in the activation free energy parameters that govern the pattern relaxation process, just as in recent experiments on relaxation of wrinkled glassy thin polymer films of variable thickness.[22] Correspondingly, recent molecular dynamics simulations of nanocomposites having variable PGNP−polymer interaction strength and PGNP concentration as well as thin polymer films of variable thickness have indicated the general occurrence of entropy−enthalpy compensation in the relaxation dynamics of these polymer materials in the high temperature Arrhenius regime accessible by simulations.[48] This study paves the way for using PGNPs as stabilizing agents for patterned structures in various applications and provides fundamental insights into how PGNPs influence the dynamics of nanocomposite materials.

Experimental Section. PMMA, M_n 3.1 kg/mol, polydispersity 1.09 was purchased from Polymer Source (P9059-MMA, syndiotactic rich content >79%) and was used as received. In situ ellipsometry measurements of our syndiotactic PMMA films indicated a depression of T_g with confinement. In particular thickness (d) dependent T_g was estimated to be approximately ≈94 °C, ≈96 °C, ≈95.6 °C, ≈96 °C, ≈96.5 °C, ≈97 °C, and ≈97 °C for a 35.5, 76, 99, 122, 187, 201, and 270 nm PMMA film, respectively. From this series of data, we estimated a limiting bulk glass transition for our PMMA matrix, $T_{g,bulk}$ = 97.24 (±0.23) °C (See Supporting Information, Figure S1a−h). T_g suppression (rather than the often cited increase in T_g) in highly syndiotactic PMMA films supported on a silicon wafer with a native oxide layer has been reported previously.[49,50]

TiO_2 nanoparticle (NP) (25 nm nominal diameter) were purchased from Sigma-Aldrich and used as received. TiO_2 (PMMA grafted) PGNP were synthesized using atom transfer radical polymerization (ATRP) by a "grafting from" approach from the NP surface. To this end, the synthesized phosphate ligand initiator was grafted on TiO_2 surface using phosphate ligand chemistry followed by ATRP. After polymerization, the PGNPs were characterized using Fourier-transform infrared spectroscopy (FTIR), nuclear magnetic resonance spectroscopy (NMR), ultraviolet−visible spectroscopy and thermogravimetric analysis (TGA) (Supporting Information, Figure S4−S8). The particles had an average diameter of 29.9 (±6.6) nm after grafting as measured by transmission electron microscopy (TEM). M_n of the grafted PMMA chains was measured to be 15 kg/mol using ^{1}H NMR of the cleaved PMMA from the grafted PGNP. PMMA grafting density was calculated to be ≈0.907 chains/nm^2 using organic mass loss from TGA (Supporting Information, Figure S5).[51]

PMMA solution (9% by relative mass in toluene) was mixed with the required amount of TiO_2 PGNP solution (2 mg/mL in toluene) to make different concentration of polymer−TiO_2 PGNP solutions (5%, 10%, 20%, and 30% by mass relative to the PMMA matrix). These solutions were then flow coated onto a silicon substrate (after 2 h of ultraviolet ozone treatment to clean the substrate), and the thickness of the films was 103 (±5) nm as measured by spectral reflectometry (F-20 Ultraviolet Thin Film Analyzer; Filmetrics, Inc.). Cross-linked poly(dimethylsiloxane) (PDMS) elastomer layers (thickness ≈1 mm, 15:1 curing ratio) were made by curing at 120 °C for 5 h on commercial digital video discs (Sony, DVD-R, pitch $\lambda \approx$ 750 nm, height difference $\Delta h \approx$ 135 nm). These elastomeric stamps were placed in contact with the polymer/polymer nanocomposite film and heated at 180 °C for 1 h to transfer the DVD pattern onto the thin film utilizing capillary forces. AFM micrographs for an unslumped pure PMMA film and 30% TiO_2 PGNP (by mass) film are shown in Figure S9a−d, Supporting Information. Water contact angle images for non-patterned pure PMMA film and 30% TiO_2 PGNP films annealed under a flat PDMS at 180 °C for 1 h are also shown in Figure S9e, Supporting Information. These measurements indicate similar surface characteristics suggesting no appreciable change in the surface energy by addition of PGNPs. Therefore, the thermodynamic driving force for structural decay should be similar for both neat and nanocomposite films.

Synthesis of the PMMA grafted SiO_2 NP (SiO_2 PGNP) was performed utilizing surface-initiated atom transfer radical polymerization according to the previously published procedures.[52,53] The particles had an average radius of 7.7 (±2) nm

DOI: 10.1021/acs.nanolett.8b02514
Nano Lett. 2018, 18, 7441−7447

after grafting as measured by transmission electron microscopy (TEM). The number average molecular mass (M_n) of the grafted PMMA chains was measured to be 19.4 kg/mol using GPC with a polydispersity of 1.17. PMMA grafting density was estimated to be ≈0.65 chains/nm^2 based on organic mass loss from TGA.[54]

Slumping experiments were conducted at 110 °C, 115 °C, 120 °C, 125 °C, and 130 °C . Imprinted samples were placed in a preheated vacuum oven for a prescribed amount of time and rapidly quenched to room temperature upon removal from the oven. The surface topography of the samples prior and after slumping were measured using atomic force microscopy (Dimension Icon, Bruker) operated in tapping mode. Multiple AFM scans are taken at random locations on each sample to determine the average height and standard deviation of the slumped pattern height.

■ ASSOCIATED CONTENT

Supporting Information

The Supporting Information is available free of charge on the ACS Publications website at DOI: 10.1021/acs.nanolett.8b02514.

In situ ellipsometric scans for PMMA films of varying thicknesses (35.5 nm, 76 nm, 99 nm, 122 nm, 187 nm, 201 nm, and 270 nm) shown in Figure S1a−g. Figure S1h depicts the thickness dependent T_g behavior of PMMA films and bulk limit value for the PMMA matrix used in this study. Transmission electron micrographs for as-cast and annealed (at 180 °C for 1 h) thin films for 30%, 20%, 10%, and 5% (by mass relative to the PMMA matrix) TiO_2 PGNP within PMMA are shown in Figure S2. TEM micrographs clearly indicate presence of clusters for annealed and imprinted films at 180 °C for 1 h. Slumping dynamics and transmission electron micrographs of SiO_2 PGNP system are shown in Figure S3. Synthesis and characterization details for the TiO_2 PGNP are depicted in Figure S4−S8. AFM micrographs and water contact angle measurements for a pure and a 30% TiO_2 PGNP filled film are shown in Figure S9. Preliminary pattern relaxation behavior below T_{comp} is depicted in Figure S10 where a 30% (by mass) TiO_2 PGNP filled film and neat PMMA film was slumped at 80 °C for 2.5 months. Statistical analysis of the AFM height micrograph clearly depicts that the height detected for the filled film was lower than the neat film, indicative of faster relaxation dynamics for filled films below T_{comp}. (PDF)

■ AUTHOR INFORMATION

Corresponding Authors

*(A.K.) akarim3@central.uh.edu.
*(J.F.D.) jack.douglas@nist.gov.

ORCID

Michael R. Bockstaller: 0000-0001-9046-9539
Christopher M. Stafford: 0000-0002-9362-8707
Jack F. Douglas: 0000-0001-7290-2300
Alamgir Karim: 0000-0003-1302-9374

Present Addresses

(A.K.) Department of Chemical and Biomolecular Engineering, University of Houston, Houston, TX 77204.
(J.Z.) School of Chemistry and Chemical Engineering and Institute of Physical Science and Information Technology, Anhui University, Hefei 230601, China.

Funding

A.K. and M.R.B. would like to acknowledge DOE (BES) award DE-SC0018854 for funding of this project.

Notes

Certain commercial materials and equipment are identified in the paper in order to adequately specify the experiemental details. In no case does such identification imply recommendation by the National Insititute of Standards and Technology nor does it imply that the material or equipment identified is necessarily the best available for this purpose.
The authors declare no competing financial interest.

■ ACKNOWLEDGMENTS

S.B. and A.K. would like to thank Dr. Bryan Vogt and Elizabeth Lewis for ellipsometric measurements, Sukhmanjot Kaur for contact angle measurements, Dr. Bojie Wang for helping with a few TEM measurements and Dr. Zhorro Nikolov for helping with the initial AFM measurements. S.B. and X.W. would like to thank Ren Zhang, Asritha Nallapaneni, Dr. Jayachandra Hari Mangalara and Dr. Sarang Bhaway for insightful discussions.

■ REFERENCES

(1) Devaraju, N. S. G. K.; Unger, M. A. *Lab Chip* **2012**, *12*, 4809−4815.
(2) Rogers, J. A.; Bao, Z.; Dodabalapur, A.; Makhija, A. *IEEE Electron Device Lett.* **2000**, *21* (3), 100−103.
(3) Nallapaneni, A.; Shawkey, M. D.; Karim, A. Specular and Diffuse Reflectance of Phase-Separated Polymer Blend Films. *Macromol. Rapid Commun.* **2017**, *38*, 1600803.
(4) Barbillon, G. In *Advances in Unconventional Lithography*; Kostovski, G., Ed.; InTech, 2011; pp 3−14.
(5) Teisseire, J.; Revaux, A.; Foresti, M.; Barthel, E. *Appl. Phys. Lett.* **2011**, *98* (1), 013106.
(6) Alvine, K. J.; Ding, Y.; Douglas, J. F.; Ro, H. W.; Okerberg, B. C.; Karim, A.; Lavery, K. A.; Lin-Gibson, S.; Soles, C. L. *J. Polym. Sci., Part B: Polym. Phys.* **2009**, *47*, 2591−2600.
(7) Alvine, K. J.; Ding, Y.; Douglas, J. F.; Ro, H. W.; Okerberg, B. C.; Karim, A.; Soles, C. L. *Soft Matter* **2009**, *5*, 2913−2918.
(8) Ding, Y.; Ro, H. W.; Germer, T. A.; Douglas, J. F.; Okerberg, B. C.; Karim, A.; Soles, C. L. *ACS Nano* **2007**, *1* (2), 84−92.
(9) Patrick, H. J.; Germer, T. A.; Ding, Y.; Ro, H. W.; Richter, L. J.; Soles, C. L. In *Proceedings of the SPIE Conference on Alternative Lithographic Technologies*; SPIE, 2009; Vol. *7271*
(10) Ding, Y.; Ro, H. W.; Douglas, J. F.; Jones, R. L.; Hine, D. R.; Karim, A.; Soles, C. L. *Adv. Mater.* **2007**, *19*, 1377−1382.
(11) Peng, H. G.; Kong, Y. P.; Yee, A. F. *Macromolecules* **2010**, *43*, 409−417.
(12) Tanaka, T.; Morigami, M.; Oizumi, H.; Ogawa, T.; Uchino, S.-I. *Jpn. J. Appl. Phys.* **1994**, *33* (12B), L1803−L1805.
(13) Cheng, S.; Xie, S.-J.; Carrillo, J.-M. Y.; Carroll, B.; Martin, H.; Cao, P.-F.; Dadmun, M. D.; Sumpter, B. G.; Novikov, V. N.; Schweizer, K. S.; Sokolov, A. P. *ACS Nano* **2017**, *11*, 752−759.
(14) Kao, J.; Thorkelsson, K.; Bai, P.; Rancatore, B. J.; Xu, T. *Chem. Soc. Rev.* **2013**, *42* (7), 2654−2678.
(15) Sunday, D. F.; Green, D. L. *Macromolecules* **2015**, *48*, 8651−8659.
(16) Bansal, A.; Yang, H.; Li, C.; Benicewicz, B. C.; Kumar, S. K.; Schadler, L. S. J. *J. Polym. Sci., Part B: Polym. Phys.* **2006**, *44*, 2944−2950.
(17) Wu, F.; Zhang, S.; Chen, Z.; Zhang, B.; Yang, W.; Liu, Z.; Yang, M. *Polymer* **2016**, *90*, 264−275.
(18) Roy, S.; Bandyopadhyay, D.; Karim, A.; Mukherjee, R. Interplay of Substrate Surface Energy and Nanoparticle Concentration in

DOI: 10.1021/acs.nanolett.8b02514
Nano Lett. 2018, 18, 7441−7447

Suppressing Polymer Thin Film Dewetting. *Macromolecules* **2015**, *48*, 373−282.
(19) Akcora, P.; Kumar, S. K.; Moll, J.; Lewis, S.; Schadler, L. S.; Li, Y.; Benicewicz, B. C.; Sandy, A.; Narayanan, S.; Ilavsky, J.; Thiyagarajan, P.; Colby, R. H.; Douglas, J. F. *Macromolecules* **2010**, *43*, 1003−1010.
(20) Zhang, R.; Lee, B.; Stafford, C. M.; Douglas, J. F.; Dobrynin, A. V.; Bockstaller, M. R.; Karim, A. *Proc. Natl. Acad. Sci. U. S. A.* **2017**, *114* (10), 2462−2467.
(21) Schadler, L. S.; Kumar, S. K.; Benicewicz, B. C.; Lewis, S. L.; Harton, S. E. *MRS Bull.* **2007**, *32*, 335−340.
(22) Chung, J. Y.; Douglas, J. F.; Stafford, C. M. *J. Chem. Phys.* **2017**, *147* (1−8), 154902.
(23) Baschnagel, J.; Okun, K.; Wolfgardt, M.; Binder, K. *Phase Transitions* **1998**, *65* (1), 263−278.
(24) Chremos, A.; Douglas, J. F. *Ann. Phys.* **2017**, *529* (5), 1600342.
(25) Hoshino, T.; Murakami, D.; Tanaka, Y.; Takata, M.; Jinnai, H.; Takahara, A. *Phys. Rev. E* **2013**, *88* (3), 032602.
(26) Liu, S.; Senses, E.; Jiao, Y.; Narayanan, S.; Akcora, P. *ACS Macro Lett.* **2016**, *5*, 569−573.
(27) Betancourt, B. A. P.; Douglas, J. F.; Starr, F. W. *J. Chem. Phys.* **2014**, *140* (20), 204509.
(28) Xu, W.-S.; Douglas, J. F.; Freed, K. F. *J. Chem. Phys.* **2016**, *145* (1−9), 234509.
(29) Zhao, J.; Simon, S. L.; McKenna, G. B. *Nat. Commun.* **2013**, *4*, 1783−1786.
(30) Novikov, V. N.; Sokolov, A. P. *Phys. Rev. E* **2015**, *92* (1−8), 062304.
(31) Ding, Y.; Sokolov, A. P. *Macromolecules* **2006**, *39* (9), 3322−3326.
(32) Seow, C. C.; Cheah, P. B.; Chang, Y. P. *J. Food Sci.* **1999**, *64* (4), 576−581.
(33) Psurek, T.; Soles, C. L.; Page, K. A.; Cicerone, M. T.; Douglas, J. F. *J. Phys. Chem. B* **2008**, *112*, 15980−15990.
(34) Waring, C. E.; Becher, P. *J. Chem. Phys.* **1947**, *15* (7), 488−496.
(35) Riggleman, R. A.; Douglas, J. F.; de Pablo, J. J. *Soft Matter* **2010**, *6*, 292−304.
(36) Anopchenko, A.; Psurek, T.; Vanderhart, D.; Douglas, J. F.; Obrzut, J. *Phys. Rev. E* **2006**, *74* (3), 031501.
(37) Cicerone, M. T.; Douglas, J. F. *Soft Matter* **2012**, *8*, 2983−2991.
(38) He, X.; Bischof, J. C. *Crit. Rev. Biomed. Eng.* **2003**, *31* (5−6), 355−422.
(39) Sun, W. Q. *Plant Physiol.* **2000**, *124*, 1203−1215.
(40) Bennett, C. A.; Kistler, R. S.; Nangia, K.; Al-Ghawas, W.; Al-Hajji, N.; Al-Jemaz, A. *Heat Transfer Eng.* **2007**, *RPS* (7), 32−42.
(41) Delcambre, S. P.; Riggleman, R. A.; de Pablo, J. J.; Nealey, P. F. *Soft Matter* **2010**, *6*, 2475−2483.
(42) Cais, R. E.; Nozomi, M.; Kawai, M.; Miyake, A. *Macromolecules* **1992**, *25* (18), 4588−4596.
(43) Einstein, A. *Investigations on the theory of the Brownian movement*, 1st ed.; Furth, R., Ed.; Dover Publications, 1956.
(44) Bicerano, J.; Douglas, J. F.; Brune, D. A. *J. Macromol. Sci., Polym. Rev.* **1999**, *39* (4), 561−642.
(45) Mackay, M. E.; Dao, T. T.; Tuteja, A.; Ho, D. L.; Van Horn, B.; Kim, H.-C.; Hawker, C. *Nat. Mater.* **2003**, *2*, 762−766.
(46) Goldansaz, H.; Goharpey, F.; Afshar-Taromi, F.; Kim, I.; Stadler, F. J.; Van Ruymbeke, E.; Karimkhani, V. *Macromolecules* **2015**, *48*, 3368−3375.
(47) Ding, Y.; Pawlus, S.; Sokolov, A. P.; Douglas, J. F.; Karim, A.; Soles, C. L. *Macromolecules* **2009**, *42*, 3201−3206.
(48) Hanakata, P. Z.; Betancourt, B. A.; Douglas, J. F.; Starr, F. W. In *Polymer Glasses*; Roth, C. B., Ed.; Taylor & Francis Group, 2016.
(49) Grohens, Y.; Hamon, L.; Reiter, G.; Soldera, A.; Holl, Y. *Eur. Phys. J. E: Soft Matter Biol. Phys.* **2002**, *8*, 217−224.
(50) Grohens, Y.; Brogly, M.; Labbe, C.; David, M. O.; Schultz, J. *Langmuir* **1998**, *14* (11), 2929−2932.
(51) Kobayashi, M.; Matsuno, R.; Otsuka, H.; Takahara, A. *Sci. Technol. Adv. Mater.* **2006**, *7*, 617−628.
(52) Pyun, J.; Matyjaszewski, K. *Chem. Mater.* **2001**, *13*, 3436−3448.
(53) Matyjaszewski, K.; Tsarevsky, N. V. *Nat. Chem.* **2009**, *1* (4), 276−288.
(54) Schmitt, M.; Zhang, J.; Lee, J.; Lee, B.; Ning, X.; Zhang, R.; Karim, A.; Davis, R. F.; Matyjaszewski, K.; Bockstaller, M. R. *Sci. Adv.* **2016**, *2* (12), No. e1601484.

DOI: 10.1021/acs.nanolett.8b02514
Nano Lett. 2018, 18, 7441−7447